Phys. Status Solidi B **247**, No. 7, 1778–1785 (2010) / **DOI** 10.1002/pssb.200945519

physica status solidi b
www.pss-b.com
basic solid state physics

Shallow-donor impurity in coupled $GaAs/Ga_{1-x}Al_xAs$ quantum well wires: hydrostatic pressure and applied electric field effects

E. Tangarife[*] and C. A. Duque

Instituto de Física, Universidad de Antioquia, AA 1226, Medellín, Colombia

Received 7 November 2009, revised 26 January 2010, accepted 10 February 2010
Published online 6 April 2010

Keywords III–V semiconductor, pressure effects, quantum well wires

[*] Corresponding author: e-mail ffranco04@gmail.com

In this work we study the binding energy of the ground state for hydrogenic donor impurity in laterally coupled $GaAs/Ga_{1-x}Al_xAs$ double quantum well wires, considering the effects of hydrostatic pressure and under the influence of a growth-direction applied electric field. We have used a variational method and the effective mass and parabolic band approximations. The low dimensional structure consists of two quantum well wires with rectangular transversal section coupled by a central $Ga_{1-x}Al_xAs$ barrier. In the study of the effect of hydrostatic pressure, we have considered the $\Gamma - X$ crossover in the $Ga_{1-x}Al_xAs$ material, which is responsible for the reduction of the height of the confining potential barriers. Our results are reported for several sizes of the structure (transversal sections of the wires and barrier thickness), and we have taken into account variations of the impurity position along the growth-direction of the heterostructure, together with the influence of applied electric fields. The main findings can be summarized as: (i) for symmetric quantum-well wires (QWW) the binding energy is an even function of the growth-direction impurity position and this even symmetry breaks in the case of asymmetric structures; (ii) the coupling between the two parallel wires increases with the hydrostatic pressure due to the negative slope of the confinement potential as a function of pressure; (iii) for impurities in the central barrier the binding energy is an increasing function of the hydrostatic pressure; (iv) depending on the direction of the applied electric field and the fixed impurity position, the binding energy can behave as an increasing or decreasing step function of the applied electric field, and finally (v) for appropriate values of the wires and barrier widths the results reproduce the exact limits of 2D and 3D hydrogenic atom as well as the limits of finite and infinite potential barrier quantum wells.

© 2010 WILEY-VCH Verlag GmbH & Co. KGaA, Weinheim

1 Introduction Pioneering works in the experimental field as the ones performed by Esaki and Tsu [1], together with those on theoretical aspects as it is the case of Bastard's study [2], opened the door to the possibility of varying the effective gap in semiconductor materials. This is accomplished by achieving a condition of quantum confinement for charge carriers. The main examples of these confined systems are the so-called semiconductor heterostructures. In this group one can find structures such as quantum wells (QW), QWW, and quantum dots (QD). All this has great implications for the technology of data storage and reading, and for the (electrical and/or optical) transmission of information.

It is long known that by doping a semiconductor with donor and/or acceptor impurities new electronic states appear in the energy spectrum. They lie within the gap of the semiconductor, thereby decreasing the width of the forbidden energy gap in it. Alternatively, when low dimensional systems such QW, QWW, and QD are built via the coupling of semiconductors with different energy gap, the effective forbidden energy region of the semiconductor becomes enlarged.

On the other hand, effects such as hydrostatic pressure, electric and/or magnetic fields, excitation by cw-laser radiation, *etc*. can be used to modulate the optical properties and the electronic and/or impurity states in such heterostructures. Taking the case of GaAs as an example, application of hydrostatic pressure results in both the augment of the energy gap and the conduction band effective mass as well as in a decrease and the static dielectric constant of the material. This means for example the occurrence of a blueshift in absorption and photoluminescence spectra [3, 4], and also the increase in the binding energy of the confined excitons [5] and donor impurities [6, 7]. In addition, one may find consequences like the appearance of red and blue shifts in the photoionization cross section associated with confined impurities in the heterostructures [8–10]; and the increasing

© 2010 WILEY-VCH Verlag GmbH & Co. KGaA, Weinheim

of the in-plane resistivity of the two-dimensional electron gas in delta-doped systems [11]. High enough applied pressure leads a type I heterostructure to become a type II one, giving the possibility of associating the minimum energy in the photoluminescence spectra either to spatially direct or indirect exciton transitions. Among the various physical parameters of doped and un-doped GaAs the optical-absorption edges and their dependence of pressure are of particular interest. Using diamond-anvil-cell techniques and high-pressure photoluminescence, Wolford and Bradley [12] and Leroux et al. [13] have investigated experimentally the low-energy optical gaps for pressure extended up to the first structural transition near 17 GPa. Useful information such as the direct--indirect character of the optical transitions can be obtained by tuning the energy levels with pressure through the Γ–X conduction-band crossover due to the very different pressure coefficients of the conduction-band minima at the Γ and X points of the Brillouin zone [14, 15].

Many authors have studied the effect of the Γ–X crossover on the optical properties associated with excitons and impurities in GaAs QW and InAs/GaAs self-assembled QD [16–26]. The studies have shown a good agreement with experimental results for the pressure coefficient of the photoluminescence peak transitions. The works of González et al. [27] and Kasapoglu et al. [9, 28] associated with impurities in QW and QWW have shown that the binding energy increases linearly with hydrostatic pressure in the direct gap regime and for pressures above the crossing between the Γ and X conduction band minima – for the barrier material –, the binding energy grows to a maximum and then decreases. The latter behavior is due to the lowering of the effective potential that confines the carriers in the region of the QW, QWW, or QD.

An applied electric field can reduce the effective energy gap in systems consisting of single QW, QWW, and QD; with the consequent redshift of the photoluminescence and absorption spectra. In the case of heterostructures composed by coupled not symmetrical systems (for example coupled QW), depending on the direction of the applied electric field it is possible to observe a redshift or a blueshift of the spectra [29, 30]. Butov et al. and Parlangeli et al. [16–19] have studied the effects of an electric field on the spatially direct and indirect transitions in coupled QW. They have also considered the effects of magnetic fields and have shown that the recombination time of exciton pairs can increase by several orders of magnitude, when crossed fields are used. de Dios-Leyva et al. [31, 32] have calculated the effects of crossed electric and magnetic fields in GaAs double QW and have shown a direct connection between the direction along which the fields are applied and the electric field values for which the first anticrossing between the two lowest-energy structures of photoluminescence spectra occurs. Studies on the effects of electric fields on impurity states in QD with different geometries and confinement profiles have revealed that the optical properties of impurity states in such systems are strongly affected by the magnitude of the confinement and the strength of the applied electric field [33–35].

A variety of studies have been reported on the combined effects of electric and magnetic fields on impurity states in QWW with different geometries [36–38]. Coaxial QWW have been considered with circular and rectangular cross sections, and rectangular (abrupt potential barriers) and parabolic potential barriers with on-axis and off-axis donor and/or acceptor impurities have been taken into account. In general, these works have been performed within the effective mass approximation (EMA) and using variational methods with trial functions depending on one and two variational parameters.

In the framework of the EMA and using the Landau-Pekar variational method, Vartanian et al. [39, 40] have presented a study of the shallow donor impurity binding energy in a rectangular QWW in the presence of a uniform electric field by taking into account the electron–longitudinal optical (LO) phonon interaction. They have shown that the electron–LO phonon interaction may strongly influence the impurity binding energy in the presence of the electric field and that for narrow GaAs QWW, the contribution of electron–phonon interaction to the impurity binding energy may be up to 10%. Erdogan et al. [41] have also applied the EMA and, with a variational procedure they calculated the effect of both electric and magnetic fields on the ground state binding energy and the self-polarization of a donor impurity in square and cylindrical infinite QWWs. Their work shows that in the high-energy regime the binding energy is only slightly sensitive, but the self-polarization is insensitive, to the magnetic field strength.

Again, a variational procedure within the EMA allowed Bai and Liu [42], and Liu et al. [43] to investigate the effect of compressive stress on the binding energies of shallow-donor impurity states in symmetrical GaAs/AlGaAs double QWW and QD with finite potential barrier height. The stress was applied in the x direction (the growth-direction of the structure) and the donor ion was located at various positions along the x-axis. Their calculations have included the crossover between the Γ- and X-conduction bands. As a general feature, they observed that the coupling effects become strong when the barrier widths become small, for fixed applied stress.

Stimulated by the work of Bai and Liu [42] the present research is concerned with a theoretical study of the combined effects of hydrostatic pressure and applied electric field on the binding energy of a shallow-donor impurity in coupled GaAs/$Ga_{1-x}Al_xAs$ QWW with finite confinement potential and rectangular transversal section. The effective-mass and parabolic band approximations have been considered within a variational procedure. The paper is organized as follows: in Section 2 we describe the theoretical framework, Section 3 is dedicated to the results and discussion, and finally, our conclusions are given in Section 4.

2 Theoretical framework

In Fig. 1 we present a pictorial view of the coupled double GaAs/$Ga_{1-x}Al_xAs$ QWW under study. The dimensions of the transversal section of the two coupled QWW as well as the width of the

© 2010 WILEY-VCH Verlag GmbH & Co. KGaA, Weinheim

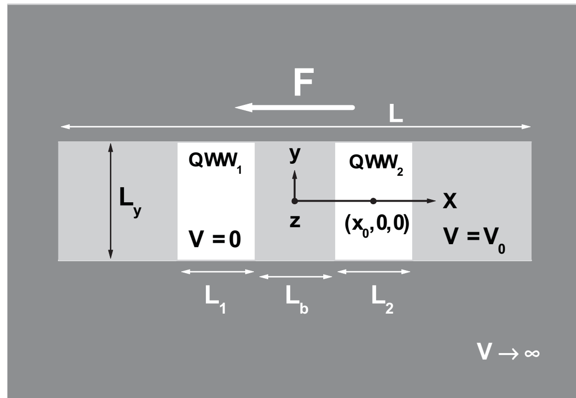

Figure 1 Pictorial view of the rectangular-transversal section GaAs/$Ga_{1-x}Al_xAs$ double QWW discussed in this work. The transversal dimensions of the wires and the central coupling barrier are shown. Also, the directions of the applied electric field and the confinement potentials, for each region of the space, are defined.

central barrier are depicted. The (x, y)-dependence of the confinement potential is denoted by different intensities of the gray color. The electric field is applied along the x-growth-direction of the heterostructure. In the effective mass and parabolic bands approximations, the Hamiltonian for a donor impurity in a couple double GaAs/$Ga_{1-x}Al_xAs$ QWW under the combined effects of hydrostatic pressure (P) and in-growth-direction applied electric field ($\vec{F} = -F\hat{x}$) is given by

$$\hat{H} = \frac{\hat{\vec{p}}^2}{2m_e^*(P)} - eFx + V(x, y, P) - \frac{e^2}{\varepsilon(P)r}, \tag{1}$$

where $\hat{\vec{p}}$, $r(=\sqrt{(x-x_0)^2 + y^2 + z^2})$, $m_e^*(P)$, and $V(x, y, P)$ are the momentum operator, the electron-impurity distance [coordinates (x, y, z) and (x_0, 0, 0) correspond to the electron and impurity positions, respectively], the hydrostatic-pressure-dependent conduction effective mass, and the hydrostatic-pressure-dependent confining potential, respectively. e is the absolute value of the electron charge and $\varepsilon(P)$ is the hydrostatic-pressure-dependent static dielectric constant for the GaAs material. For the confinig potential, $V_0(P)$, we use the 60% of the hydrostatic-pressure-dependent barrier-well band-offset. The pressure dependencies of the conduction effective mass, GaAs static dielectric constant, and confinement potential (in meV) are given, respectively, by Refs. [7, 44]

$$m_e^*(P) = \left(0.0665 + 5.60 \times 10^{-4}\ \text{kbar}^{-1}P\right)m_0, \tag{2}$$

$$\varepsilon(P) = 12.6273 - 0.0088\ \text{kbar}^{-1}P, \tag{3}$$

and

$$V_0(P) = \begin{cases} 257 - 0.01\ \text{kbar}^{-1}P, & P \leq 9.57\ \text{kbar}, \\ 316 - 5.02\ \text{kbar}^{-1}P \\ \quad - 0.12\ \text{kbar}^{-2}P^2, & P > 9.57\ \text{kbar}, \end{cases} \tag{4}$$

where m_0 is the free electron mass and P is given in kbar.

The wave function for the impurity ground state and its corresponding energy are obtained by means of a variational procedure which minimizes the energy functional:

$$E(\lambda) = \frac{\langle\Phi(x, y, z)|\hat{H}|\Phi(x, y, z)\rangle}{\langle\Phi(x, y, z)|\Phi(x, y, z)\rangle}, \tag{5}$$

where λ is the variational parameter and the trial wave function, $\Phi(x, y, z)$, is

$$\Phi(x, y, z) = Nf(x)\cos\left(\pi y/L_y\right)e^{-\lambda r}. \tag{6}$$

Here $e^{-\lambda r}$ represents a 1s-like hydrogenic wave function, and $f(x)/g(y)[=\cos\left(\pi y/L_y\right)]$ is the eigenfunction (with eigenvalue E_x/E_y) of the x/y-dependent part of the Hamiltonian in Eq. (1), without the impurity potential term at the right. Here we follow the work by Xia and Fan [45] and write $f(x)$ as

$$f(x) = \left(\frac{1}{L}\right)^{\frac{1}{2}} \sum_{m=1}^{\infty} C_m \sin\left(\frac{2m\pi x}{L} + \frac{m\pi}{2}\right). \tag{7}$$

The impurity binding energy is obtained by the usual definition

$$E_b = E_x + E_y - E(\lambda)|_{\min}. \tag{8}$$

3 Results and discussion

In what follows, all the results are reported for $L_y = 10$ nm; the simplified notation (L_1, L_b, L_2), with $L_C = L_1 + L_b + L_2$, will be used when making reference to the dimensions of the double QWW system.

In Fig. 2 we show the binding energy as a function of hydrostatic pressure. We have separated the effects of hydrostatic pressure individually. The curve denoted by E_a corresponds to the binding energy under the effects of hydrostatic pressure only on the confinement potential $V_0(P)$ with constant values of effective mass m^* and dielectric constant ε —the binding energy reflects a linear behavior

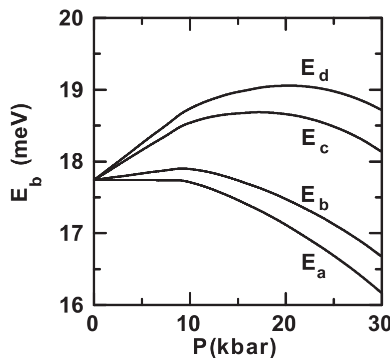

Figure 2 Binding energy as a function of the hydrostatic pressure for a donor impurity in a GaAs/$Ga_{0.7}Al_{0.3}As$ double QWW. The result is for (10, 1, 10) nm. The impurity is located at the center of the right-hand wire (see Fig. 1).

© 2010 WILEY-VCH Verlag GmbH & Co. KGaA, Weinheim

approximately constant until $P = 9.57$ kbar and for greater pressures a decreasing behavior as expected by considering Eq. (4). The curve E_b shows in a combined way the effects of hydrostatic pressure on the dielectric constant and the confinement potential leaving constant the effective mass. The results reflect an increase in the binding energy due to the decrease in the dielectric constant and thus an increase in the Coulomb interaction term. The curve E_c shows in a combined way the effects of hydrostatic pressure on the effective mass and the confinement potential leaving constant the dielectric constant. Again, the results reflect an increase in the binding energy, due to the increase in the effective mass with the hydrostatic pressure. The curve E_d shows simultaneously the effects of hydrostatic pressure on the effective mass, the dielectric constant, and the confinement potential, indicating the pronounced increase in the binding energy due to the overlap of the individual effects. Table 1 shows the quadratic adjustments with hydrostatic pressure of the binding energy curves in Fig. 2. The curve E_d corresponds to the overlap of the curves E_b and E_c ($E_d = E_b + E_c$), that is to say, the combination of the effects of the hydrostatic pressure on the effective mass and the dielectric constant is the sum of their individual effects. We validate this claim by the linear coefficients of the adjustment, since it holds that $\alpha_d = \alpha_b + \alpha_c - \alpha_a$. Besides, clearly we observe that $\alpha_c > \alpha_b$, showing thus that the influence of the hydrostatic pressure on the effective mass has predominant effects on the binding energy compared to the influence of the hydrostatic pressure on the dielectric constant.

The results for the binding energy of a donor impurity in a GaAs/$Ga_{0.7}Al_{0.3}$ asymmetric double QWW as a function of the width of the central barrier (L_b) are shown in Fig. 3. In the case of zero electric field [Fig. 3(a)], as long as L_b increases the binding energy augments. In this situation the wave function is concentrated near to the impurity site (the center of the right-hand wire QWW_2), decreasing the expectation value of the electron-impurity distance along the x-direction [$D_x = \langle\Phi(x,y,z) \parallel x - x_0 \parallel \Phi(x,y,z)\rangle$]. The almost constant region of values of E_b, shown for large enough values of the interwell barrier width, is due to the fact that the probability to find the electron in the left wire is approximately zero. The final increase of the binding energy for L_b near 40 nm and above comes from to the interaction with the infinite potential barriers in $x = +L/2$ (see Fig. 1). A rise of P from 0 to 15 kbar causes the GaAs effective mass

Table 1 Quadratic adjustments of the binding energy curves in Fig. 2 as a function of hydrostatic pressure ($E_i = E_{0i} + \alpha_i P + \beta_i P^2$).

E_i (meV)	E_0 (meV)	α (kbar^{-1})	β (kbar^{-2})
E_a	17.73	0.017	−0.002
E_b	17.73	0.037	−0.002
E_c	17.70	0.116	−0.003
E_d	17.69	0.136	−0.003

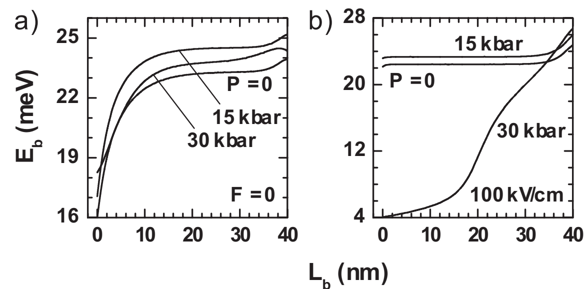

Figure 3 Binding energy as a function of the width of the central barrier for a symmetric GaAs/$Ga_{0.7}Al_{0.3}$As double QWW of dimensions $(10, L_b, 10)$ nm. The impurity is located at the center of the right-hand wire (see Fig. 1). The binding energy is calculated for several values of the hydrostatic pressure and applied electric field. (a) $F = 0$, (b) $F = 100$ kV/cm.

increases and the dielectric constant to fall, resulting in an increase in the confinement of the carriers and in the Coulomb interaction, which is reflected in the increment of the binding energy observed in the figure (see above the discussion of Fig. 2). But if P reaches the value of 30 kbar, then the values of the binding energy turn to be lower. In fact, what we have for $P > 9.57$ kbar is a considerable decrease of $V_0(P)$, making the system less confined and therefore the binding energy goes down. It is observed that for $L_b \to 0$ the binding energy is higher as the hydrostatic pressure is higher, mainly due to the increase in the confinement of the carriers and also, but with lesser influence, in the Coulomb interaction with the hydrostatic pressure. Furthermore, if an external applied electric field with strength equals to 100 kV/cm is considered [Fig. 3(b)], the situation changes as follows. The approximately constant behavior of the binding energy as a function of L_b, in the case of $P = 0$, is due to the displacement of the wave function toward the proximities of the impurity. That is, the wave function strongly localizes within the QWW_2 region. For $P = 15$ kbar the effective mass increases and the dielectric constant decreases and, consequently, the carrier confinement, the Coulomb interaction, and the binding energy increase. If finally the hydrostatic pressure is raised up to $P = 30$ kbar there will be a considerable decrease in $V_0(P)$, allowing that the applied electric field pushes the wave function to the barrier region between $L_b/2 + L_2 < x < +L/2$, thus increasing D_x. As a consequence, E_b diminishes. The growing behavior observed when L_b increases is explained by realizing that the impurity is now located in the region for which the electron amplitude of probability is maximum. Then D_x decreases, leading to the increase in the E_b. As commented above for in Fig. 3(a), the final augment in the binding energy curves are due to the interaction with the infinite potential barriers at $x = +L/2$.

Figure 4 shows the results for the binding energy of a donor impurity in a GaAs/$Ga_{0.7}Al_{0.3}$As symmetric double QWW as a function of the wire width, $L_w = L_1 = L_2$, for different combinations of hydrostatic pressure and applied electric field. For small L_w values the wave function is

© 2010 WILEY-VCH Verlag GmbH & Co. KGaA, Weinheim

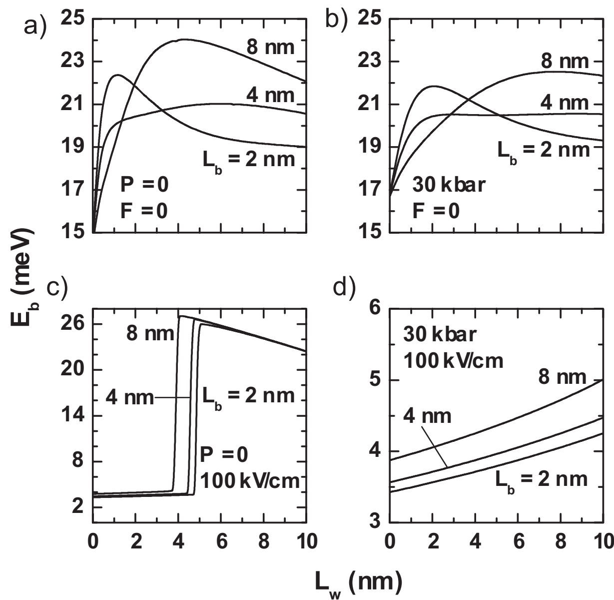

Figure 4 Binding energy of a donor impurity in a symmetric GaAs/$Ga_{0.7}Al_{0.3}As$ double QWW of dimensions (L_w, L_b, L_w) nm. The results are as a function of the width of the wire and for several values of the width of the central barrier. The impurity is located at the center of the right-hand wire (see Fig. 1). The binding energy is calculated for different values of hydrostatic pressure and applied electric field.

confined by the presence of the potential barriers in its proximity, with the corresponding increase of the binding energy. There is a critical value for the wire and central barrier widths for which the binding energy reaches a maximum; such values correspond to the optimum setting for which the wave function penetrates very little in the regions of the barrier. If $L_w \to 0$ the binding energy tends to – approximately – the limit of the binding energy of an infinite QW of width $L_y = 10$ nm at $P = 0$ (≈ 14.3 meV as previously obtained [7]). The decrease in the binding energy for large values of L_w is due to the fact that the wave function spreads along the entire wire width. In Fig. 4(a), for $L_w > 2$ nm, when $L_b = 8$ nm it can be observed that the binding energy is larger than in the case of $L_b = 2$ nm. This is due to the fact that for larger barriers the two QWW become uncoupled, causing that the electron is essentially confined in the region of the impurity site. When applying a finite hydrostatic pressure, Fig. 4(b), we can discuss two separately influencing effects once again: (i) the effective mass is an increasing function of the hydrostatic pressure, with the increasing of the carriers confinement, and the dielectric constant is a decreasing function of the hydrostatic pressure, with the increasing of the Coulomb interaction strength; (ii) the confinement potential $V_0(P)$ is a decreasing function of the hydrostatic pressure. In the regime of small L_w values, this second effect is dominant over the first one. For that reason, it is now seen that the curves of the binding energy as a function of L_w show a smaller slope till the corresponding maximum. For large L_w, the binding energy increases (compared to the binding energy without hydrostatic pressure) due to an increase in the carriers confinement and in the electrostatic interaction, being the effects associated with the effective mass the dominant over the confinement potential effects (see above the discussion of Fig. 2). For $L_w \to 0$ the binding energy is approximately in the limit of the binding energy of on-center donor impurity in an infinite QW of width $L_y = 10$ nm at $P = 30$ kbar (≈ 17.4 meV [7]). There is also a set of critical values for the widths of wire and central barrier for which the binding energy reaches a maximum. Such values are displaced toward the right with respect the associated ones for zero P. Again, this behavior is associated with the decrease of $V_0(P)$. Applying an electric field to the system, Fig. 4(c), results in an increasing of D_x with the corresponding decrease in the binding energy. This configuration of applied electric field pushes the electron wave function to the limit of the infinite potential at $x = +L/2$. There is an specific value of L_w for which the electron wave function is confined in the proximity of the impurity. For higher values of such width the wave function spreads all over the transversal section of the wire increasing D_x, thus reflecting the final decrease of the binding energy. When considering – in a combined way – the effects of hydrostatic pressure and electric field, Fig. 4(d); it can be observed a rising in the binding energy as long as L_w grows. Due to the hydrostatic pressure the carrier confinement and the electrostatic interaction increases and the confinement potential falls. Because of the applied electric field, the wave function is shifted far from the impurity site with the corresponding increasing of D_x. By enhancing the wire widths, there is an approach between the impurity site and the point where the square modulus of the wave function has its maximum, with the consequent decrease of D_x, leading to an increase in the binding energy.

The dependencies of the donor binding energy upon the x-impurity position in rectangular-transversal section GaAs/$Ga_{0.7}Al_{0.3}As$ double QWW are shown in Figs. 5 and 6 for $F = 0$ and $F = 100$ kV/cm, respectively. Two values of the hydrostatic pressure have been considered: $P = 0$ (a) and $P = 30$ kbar (b). The lines 1 and 2 correspond, respectively, to symmetrical and asymmetrical settings of the dimensions of the double QWW. In (c) and (d) it is shown the square module of the x-dependent wave function $f(x)$. Let us, first, concentrate our attention on the case of $F = 0$ (Fig. 5). It can be seen that when the system is symmetric (1), $|f(x)|^2$ is also symmetric, indicating that the electron can be found in any of both QWWs. On the other hand, when the system is asymmetric (2), $|f(x)|^2$ is asymmetric as well, indicating that the electron is essentially located in the QWW of largest transversal section. In Fig. 5(a), the binding energy is presented as a function of the x-impurity position. In the case of the symmetric structure (line 1) as the impurity moves along the QWW_1 region, the maximum of the electron wave function locates in the proximity of the impurity, reflecting the highest value of the binding energy there (where it is higher the probability of finding the electron). When the impurity is in the barrier region, D_x grows and the binding

© 2010 WILEY-VCH Verlag GmbH & Co. KGaA, Weinheim

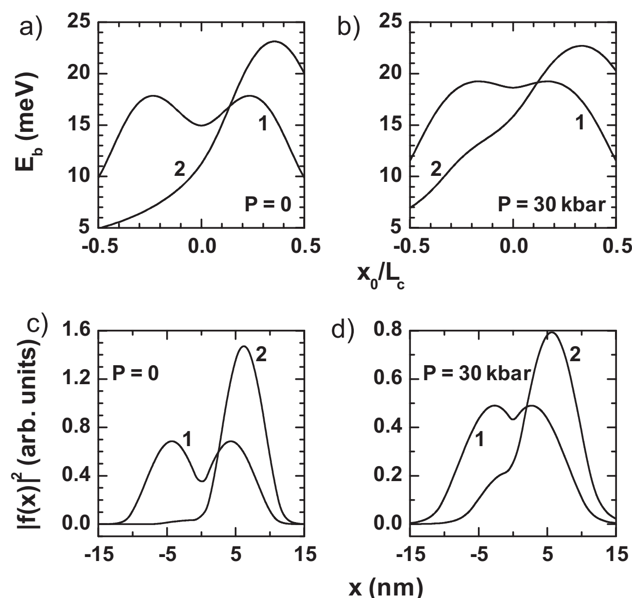

Figure 5 (a) and (b) Binding energy as a function of the impurity position in a symmetric $GaAs/Ga_{0.7}Al_{0.3}As$ double QWW. The results are for two values of the hydrostatic pressure with $F = 0$ and for (10, 1, 10) nm (line 1) and (5, 2.5, 10) nm (line 2). (c) and (d) are for $|f(x)|^2$ for two different values of the hydrostatic pressure with lines 1 and 2 having the same meaning such as in Figs. (a) and (b).

energy decreases. When the impurity enters to the QWW_2 region the wave function is again located in the proximity of the impurity, once more reflecting the highest value of binding energy. The symmetry in the binding energy is a consequence of the symmetry of $|f(x)|^2$. For the case of asymmetric structure (line 2), the predominant location of the wave function in the QWW_2 region implies a higher maximum of the binding energy; providing the binding energy with an asymmetric behavior as a consequence of the asymmetry in $|f(x)|^2$.

The application of hydrostatic pressure to the system [Fig. 5(b)] reduces considerably the value of $V_0(P)$ allowing the wave function to spread along the whole heterostructure [see Fig. 5(d)]. Consequent with the decreasing of $V_0(P)$, there is an increasing of $|f(x)|^2$ in the central barrier which finally reflects in higher values of the binding energy for impurities located in the barrier region. In other words, the hydrostatic pressure strongly couples the two QWW. If we now we go on the case of $F = 100$ kV/cm (Fig. 6), it can be seen that for both configurations – symmetric (line 1) and asymmetric (line 2) – the electron is essentially in the QWW_2 region and in consequence the binding energy is largest/lowest for impurities in the QWW_2/QWW_1 region [see Fig. 6(a)]. Applying hydrostatic pressure to the system reduces considerably $V_0(P)$. This allows the wave function to be polarized and displaced by the electric field outside of the region of the double QWWs and toward the finite barrier in the region $L_b/2 + L_2 < x < +L/2$ [see Fig. 6(d)]. As the impurity is displaced inside the heterostructure, D_x decreases, thus increasing the value of the binding energy when the impurity moves toward the QWW_2 region.

In Fig. 7 are depicted the results for the dependence of the binding energy with the applied electric field and the hydrostatic pressure for a donor impurity in a rectangular-transversal section $GaAs/Ga_{0.7}Al_{0.3}As$ double QWW. The impurity is located at the center of the QWW_2 region. In Fig. 7(a) it is seen that, when increasing the electric field, the electron wave function is polarized and displaced toward the QWW_2 region, favoring the confinement of the wave function in the proximity of the impurity, which reflects in an increase in the binding energy. When the increase in the electric field continues the wave function can enter the barrier zone $L_b/2 + L_2 < x < +L/2$ provoking an increase in D_x and consequently a decrease in the binding energy. For large enough applied electric field values (≈144 kV/cm) the electron wave function reaches the infinite barrier at $+L/2$, keeping D_x constant and reflecting the constant value of the binding energy. For negative values of the applied electric field, the electron wave function polarizes and moves toward the QWW_1 region, increasing D_x and decreasing gradually the binding energy up to the limit value. With more negative values of the applied electric field, the electron wave function reaches the infinite barrier at $-L/2$, keeping D_x constant and – once again – reflecting the constant value of the binding energy. It should be noticed when observing the curves that the initial value of the binding energy is lower than the final value, due to the fact that when the electron is pushed to the infinite barrier at $-L/2$ the electron-impurity distance is larger than in the situation when the electron is pushed to the infinite barrier at $+L/2$.

Applying hydrostatic pressure, Fig. 7(b), reduces considerably $V_0(P)$ provoking a decrease in the applied electric field necessary to polarize and displace the wave function up to the infinite potential barriers at $\pm L/2$. The

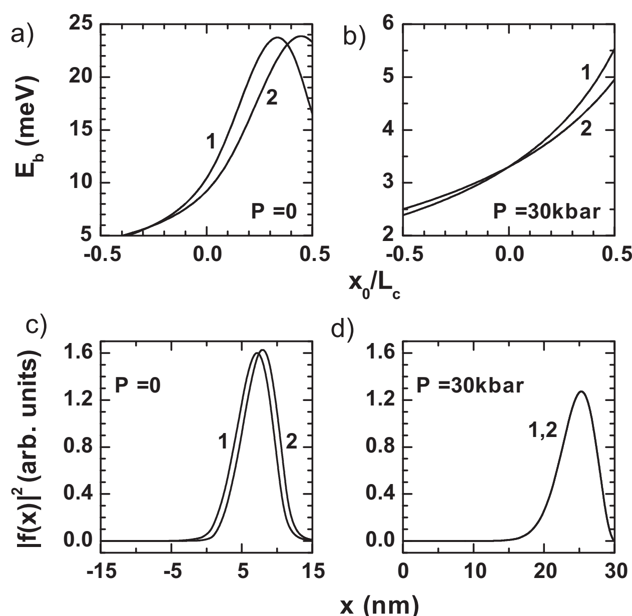

Figure 6 The results are as in Fig. 5, but for $F = 100$ kV/cm.

 © 2010 WILEY-VCH Verlag GmbH & Co. KGaA, Weinheim

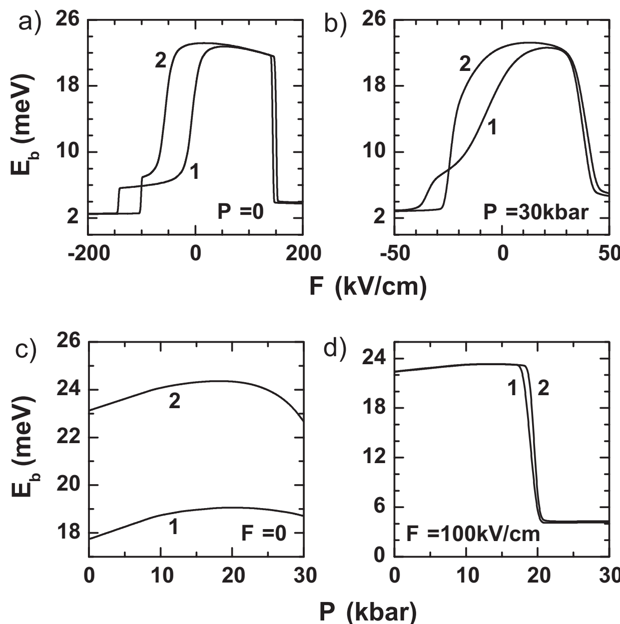

Figure 7 Binding energy as a function of the applied electric field and hydrostatic pressure for a donor impurity in a GaAs/$Ga_{0.7}Al_{0.3}As$ double QWW. The results are for (10, 1, 10) nm (line 1) and (5, 2.5, 10) nm (line 2). The impurity is located at the center of the right-hand wire (see Fig. 1).

effect of the hydrostatic pressure, Fig. 7(c), increases/reduces gradually the effective mass/dielectric constant which favors the carrier confinement/Coulomb interaction, leading to an augment of the value of the binding energy (see above the discussion of Fig. 2). For large enough values of the hydrostatic pressure (over the $\Gamma - X$ crossover in the barrier material), $V_0(P)$ is reduced considerably predominating over the term of Coulomb interaction. This is reflected in the final decrease of the binding energy. For the asymmetric setting (line 2) the predominating location of the electron wave function is in the QWW_2 region; whereas for the symmetric setting (line 1) there is the same probability in each of the wires. The value of D_x is lower in the asymmetric setting (line 2) which reflects in the higher values of E_b. The application of an electric field of 100 kV/cm, Fig. 7(d), polarizes and displaces the electron wave function toward the QWW_2 region, favoring the confinement in such region. The initial increment of the binding energy is associated with the gradual increase/decrease in the effective mass/dielectric constant with the hydrostatic pressure. In the high pressure regime (over the $\Gamma - X$ crossover in the barrier material), $V_0(P)$ is considerably reduced allowing the electron wave function to reach the infinite potential at $+L/2$, with the consequent large value of D_x. So that, there is a considerable decrease in the binding energy with constant behavior in the end of the curve.

4 Conclusions

Using a variational method and the effective mass and parabolic band approximations we have calculated the binding energy of a donor impurity in rectangular-transversal section GaAs/$Ga_{1-x}Al_xAs$ double quantum well wires under the combined effects of hydrostatic pressure and applied electric field. The impurity has been located in different regions of the transversal section of the heterostructure, which has been studied for symmetric and asymmetric configurations. Calculations have considered the hydrostatic pressure-related $\Gamma - X$ crossover for the conduction bands of the $Ga_{1-x}Al_xAs$ material. The findings can be summarized as follows: (i) for symmetric double QWW structures a symmetric behavior can be observed of the binding energy when the impurity position moves throughout the growth-direction of the heterostructure (x); and this symmetric behavior breaks in the case of asymmetric structures and can be understood in terms of the line-shape of the amplitude of probability along the x-direction; (ii) the hydrostatic pressure favors the coupling between the two QWW that compose the system; (iii) for impurities in the central barrier the binding energy is an increasing function of the hydrostatic pressure; (iv) for fixed impurity positions the binding energy behaves as increasing or decreasing step function of the applied electric field and this behavior is associated with the direction of the applied electric field and with the impurity position, and (v) for large enough values of the applied electric field, and depending of the value of the hydrostatic pressure, the information of the double QWW heterostructure is lost and the system behaves as a single rectangular-transversal section quantum QWW with infinite confinement potential barriers and transversal dimensions $L \times L_y$.

The study here presented constitutes a derivation of our previous work of impurities in coupled QW [7]. The new features under consideration here is that we have studied the coupling of QWW not only through changes in hydrostatic pressure and changes in the width of the central barriers but also by the effect of an applied electric field. Note that going from a one dimensional confinement (QW) to a two-dimensional confinement (QWW) implies an increase in the binding energy of the carriers essentially in a factor of two. The character of coupled QWW becomes in a system of two coupled QW for L_y larger than ~ 500 Å. To consider an additional confinement in the z-direction corresponds to the problem of two coupled QD. This geometry could be useful for example in the study of an exciton in a pair of laterally and/or vertically coupled QD. Finally, The results presented here would be complemented with the study of the dependence of donor impurity states upon the effect of electron–phonon interaction. A confined-optical-phonon model becomes suitable for calculating the corresponding bound-polaron corrections [46–51]. Work on this subject and also of the problem of exciton and impurity states in coupled QD is currently in progress and its results will be published elsewhere.

Acknowledgements This research was partially supported by Colombian Agencies: COLCIENCIAS, CODI-Universidad de Antioquia (Estrategia de Sostenibilidad Grupo de Materia

© 2010 WILEY-VCH Verlag GmbH & Co. KGaA, Weinheim

Condensada-UdeA, 2009-2010), and Facultad de Ciencias Exactas y Naturales-Universidad de Antioquia (CAD-exclusive dedication project 2009-2010). Authors are grateful to Dr. M. E. Mora-Ramos for useful discussions and the critical reading of the manuscript. C.A.D is also grateful to Dr. Anna Kurczyńska for useful discussions.

References

[1] L. Esaki and R. Tsu, IBM Res. Note RC-2418 (1969). L. Esaki and R. Tsu, IBM J. Res. Devel. **14**, 61 (1970).
[2] G. Bastard, Phys. Rev. B **24**, 4714 (1981).
[3] C. A. Duque, N. Porras-Montenegro, Z. Barticevic, M. Pacheco, and L. E. Oliveira, J. Phys: Condens. Matter **18**, 1877 (2006).
[4] S. Y. López, N. Porras-Montenegro, and C. A. Duque, Physica B **362**, 41 (2005).
[5] N. Raigoza, C. A. Duque, E. Reyes-Gómez, and L. E. Oliveira, Physica B **367**, 267 (2005).
[6] S. Y. López, N. Porras-Montenegro, and C. A. Duque, Semicond. Sci. Technol. **18**, 718 (2003).
[7] N. Raigoza, A. L. Morales, A. Montes, N. Porras-Montenegro, and C. A. Duque, Phys. Rev. B **69**, 045323 (2004).
[8] J. D. Correa, N. Porras-Montenegro, and C. A. Duque, Phys. Status Solidi B **241**, 2440 (2004).
[9] E. Kasapoglu, U. Yesilgül, H. Sari, and I. Sökmen, Physica B **368**, 76 (2005).
[10] M. G. Barseghyan, A. A. Kirakosyan, and C. A. Duque, Phys. Status Solidi B **246**, 626 (2009).
[11] O. Oubram, M. E. Mora-Ramos, and L. M. Gaggero-Sager, Eur. Phys. J. B **71**, 233 (2009).
[12] D. J. Wolford and J. A. Bradley, Solid State Commun. **53**, 1069 (1985).
[13] M. Leroux, J. M. Sallese, J. Leymarie, G. Neu, and P. Gibart, Semicond. Sci. Technol. **6**, 514 (1991).
[14] G. H. Li, A. R. Goñi, K. Syassen, O. Brandt, and K. Ploog, J. Phys. Chem. Solids **56**, 38S (1995).
[15] A. R. Goñi and K. Syassen, Semicond. Semimetals **54**, 247 (1998).
[16] L. V. Butov, A. A. Shashkin, V. T. Dolgopolov, K. L. Campman, and A. C. Gossard, Phys. Rev. B **60**, 8753 (1999).
[17] L. V. Butov, A. Imamoglu, A. V. Mintsev, K. L. Campman, and A. C. Gossard, Phys. Rev. B **59**, 1625 (1999).
[18] A. Parlangeli, P. C. M. Christianen, J. C. Maan, C. B. Soerensen, and P. E. Lindelof, Phys. Status Solidi A **178**, 45 (2000).
[19] A. Parlangeli, P. C. M. Christianen, J. C. Maan, I. V. Tokatly, C. B. Soerensen, and P. E. Lindelof, Phys. Rev. B **62**, 15323 (2000).
[20] J. H. Burnett, H. M. Cheong, W. Paul, E. S. Koteles, and B. Elman, Phys. Rev. B **47**, 1991 (1993).
[21] A. M. Elabsy, Superlattices Microstruct. **14**, 65 (1993).
[22] A. M. Elabsy, J. Phys.: Condens. Matter **6**, 10025 (1994).
[23] C. A. Duque, S. Y. López, and M. E. Mora-Ramos, Phys. Status Solidi B **244**, 1964 (2007).
[24] M. E. Mora-Ramos, S. Y. López, and C. A. Duque, Eur. Phys. J. B **62**, 257 (2008).
[25] I. E. Itskevich, S. G. Lyapin, I. A. Troyan, P. C. Klipstein, L. Eaves, P. C. Main, and M. Henini, Phys. Rev. B **58**, R4250 (1998).
[26] I. E. Itskevich, M. S. Skolnick, D. J. Mowbray, I. A. Trojan, S. G. Lyapin, L. R. Wilson, M. J. Steer, M. Hopkinson, L. Eaves, and P. C. Main, Phys. Rev. B **60**, R2185 (1999).
[27] J. W. González, S. Y. López, A. H. Rodríguez, N. Porras-Montenegro, and C. A. Duque, Phys. Status Solidi B **244**, 70 (2007).
[28] E. Kasapoglu, Phys. Lett. A **373**, 140 (2008).
[29] S. Y. López, M. E. Mora-Ramos, and C. A. Duque, Solid State Sci. **12**, 210 (2010).
[30] S. Y. López, M. E. Mora-Ramos, and C. A. Duque, Physica B **404**, 5181 (2009).
[31] M. de Dios-Leyva, C. A. Duque, and L. E. Oliveira, Phys. Rev. B **75**, 035303 (2007).
[32] M. de Dios-Leyva, C. A. Duque, and L. E. Oliveira, Phys. Rev. B **76**, 075303 (2007).
[33] A. L. Vartanian, L. A. Vardanyan, and E. M. Kazaryan, Phys. Lett. A **360**, 649 (2007).
[34] A. J. Peter and V. Lakshminarayana, Chin. Phys. Lett. **25**, 3021 (2008).
[35] W. Xie and Q. Xie, Physica B **404**, 1625 (2009).
[36] A. F. Terzis and S. Baskoutas, J. Phys.: Conf. Series **10**, 77 (2005).
[37] V. N. Mughnetsyan, M. G. Barseghyan, and A. A. Kirakosyan, Superlattices Microstruct. **44**, 86 (2008).
[38] S. Aktas, F. K. Boz, and S. S. Dalgic, Physica E **28**, 96 (2005).
[39] A. L. Vartanian, M. A. Yeranosyan, and A. A. Kirakosyan, Physica E **27**, 447 (2005).
[40] A. L. Vartanian, M. A. Yeranosyan, and A. A. Kirakosyan, Physica B **390**, 256 (2007).
[41] I. Erdogan, O. Akankan, and H. Akbas, Phys. E **35**, 27 (2006).
[42] Z.-G. Bai and J.-J. Liu, J. Phys.: Condens. Matter **19**, 346218 (2007).
[43] J.-J. Liu, M. Shen, and S.-W. Wang, J. Appl. Phys. **101**, 073703 (2007).
[44] A. R. Goñi, K. Syassen, and M. Cardona, Phys. Rev. B **41**, 10104 (1990).
[45] J.-B. Xia and W.-J. Fan, Phys. Rev. B **40**, 8508 (1989). We refer the reader to this work for details of the calculation of $f(x)$.
[46] F. Comas and M. E. Mora-Ramos, Physica B **159**, 413 (1989).
[47] H. Rücker, M. Mora-Ramos, and F. Comas, Phys. Status Solidi B **159**, 117 (1990).
[48] H. Rücker, M. Mora-Ramos, and F. Comas, Superlatt. Microstruct. **9**, 397 (1991).
[49] R. Riera, F. Comas, M. E. Mora-Ramos, and C. Trallero-Giner, Physica B **168**, 211 (1991).
[50] M. E. Mora-Ramos and A. Bruno-Alfonso, in: Optoelectronic Materials and Their Applications, edited by F. Leccabue, O. de Melo Pereira, and I. Hernández-Calderón (Edizioni ETS, Pisa, Italy, 1993).
[51] M. E. Mora-Ramos and D. A. Contreras-Solorio, Physica B **253**, 325 (1998).

© 2010 WILEY-VCH Verlag GmbH & Co. KGaA, Weinheim